https://doi.org/10.5194/egusphere-2025-1921
Preprint. Discussion started: 25 June 2025

Running head: Differential dissolution in coccolithophores

Species-specific differential dissolution morphology of selected coccolithophore species: an experimental study

Gerald Langer[1,2], Ian Probert[3], Jeremy R. Young[4], Patrizia Ziveri[1,5,6]

Affiliations

[1] Institute of Environmental Science and Technology, Universitat Autònoma de Barcelona (ICTA-UAB), Barcelona, 08193, Spain

[2] National Institute of Oceanography and Applied Geophysics - OGS, Trieste, 34151, Italy

[3] Sorbonne Université/CNRS, Roscoff Culture Collection, FR2424 Station Biologique de Roscoff, 29682 Roscoff, France

[4] Earth Sciences, University College London, London WC1E 6BT, UK

[5] Catalan Institution for Research and Advanced Studies (ICREA), Barcelona, Spain

[6] BABVE Dept., Universitat Autònoma de Barcelona (ICTA-UAB), Barcelona, 08193, Spain

Corresponding author: Gerald Langer (gerald.langer@cantab.net, gerald.langer@uab.cat)

500-character summary

Coccolithophores are important marine $CaCO_3$ producers and their biominerals, the coccoliths, partly dissolve in the upper water column where dissolution is unexpected. Studying coccolith dissolution in field samples is hampered by a paucity of experimental studies describing dissolution morphologies. Here we fill this gap by experimentally dissolving different coccolithophores and applying our results to field samples.

https://doi.org/10.5194/egusphere-2025-1921
Preprint. Discussion started: 25 June 2025

Highlights

- Experimental studies on biogenic $CaCO_3$ dissolution provide novel insights into field sample observations and biomineralization processes
- Experimental data aid the interpretation of aberrant coccolith morphology in field samples
- In *C. braarudii* partial dissolution reveals a nanostructure in the distal shield
- The nanostructure in *C. braarudii* requires adjustments in biomineralization models

Abstract

We conducted a laboratory $CaCO_3$ dissolution experiment to detect differential dissolution morphologies of three selected coccolithophore (abundant marine calcareous phytoplankton) species, *Coccolithus braarudii*, *Helicosphaera carteri*, and *Scyphosphaera apsteinii*. These species were selected because they are ecologically and biogeochemically important (significant contributors to $CaCO_3$ production) and have been less studied than *Gephyrocapsa*. Muroliths of *S. apsteinii* dissolve faster than lopadoliths, which in turn dissolve as fast as *H. carteri* but faster than *C. braarudii*. Lopadolith R-units dissolve faster than V-units. Comparison with field samples shows that experimental data are helpful when interpreting field samples. For example, we identify dissolution in water and sediment samples reported in the literature. In *C. braarudii* dissolution reveals a nanostructure on the proximal side of the distal shield, an observation that has implications for coccolith biomineralization models, which do not currently account for the formation of such a structure.

1) Introduction

Present anthropogenic CO_2 concentration changes, both atmospheric and marine, cannot be fully understood without considering marine calcium carbonate, largely produced by calcifying organisms (Broecker and Peng 1982, Morse and Mackenzie 1990). The most productive marine calcium carbonate ($CaCO_3$) producers are pelagic organisms, with coccolithophores contributing ca. 90% of global pelagic $CaCO_3$ production (Ziveri et al., 2023) and ca. 50% of $CaCO_3$ sedimentation (Milliman 1993,

https://doi.org/10.5194/egusphere-2025-1921
Preprint. Discussion started: 25 June 2025

Broecker and Clark 2009). Dissolution of $CaCO_3$ in the photic zone is an important process in the marine $CaCO_3$ cycle (Ziveri et al. 2023; Subhas et al. 2022; Sulpis et al. 2021). In addition to occurring in the open ocean photic zone, dissolution of carbonates in general, and coccoliths in particular, may also occur in sediments and coastal CO_2 vent sites (Honjo 1975, Ziveri et al 2014).

Assessing coccolith dissolution in these diverse settings can be challenging, but partial dissolution morphologies as identified in electron micrographs have proved a useful tool (e.g. Langer et al 2007, Ziveri et al 2014). The interpretation of field samples is difficult, however, because the degree, and even the mere fact, of dissolution often need to be inferred from the micrographs alone, without precise knowledge of the physico-chemical conditions leading to the observed morphology. The first task is to distinguish dissolution from malformation and the second task is to assess the degree of dissolution. *Calcidiscus leptoporus* coccoliths (placoliths characterized by two shield-like plates connected by a central tube) lacking proximal shields have been observed in surface sediments, leading to the conclusion that single shields are a sign of heavy dissolution (Roth and Berger 1975), which has been proposed as a proxy for dissolution in the sedimentary record (Matsuoka 1999). Only an experimental study could show that separation of the shields is the first observable dissolution feature occurring at less than 8% mass loss (Langer et al 2007). The latter study, in addition to aiding the interpretation of field samples, revealed structural features unobservable in standard scanning electron microscope (SEM) observations, i.e. the “weak spot” at the proximal end of the tube (the position of the proto-coccolith ring, Young et al 2004) leading to shield separation at the first stages of dissolution.

Despite the importance of experimental studies showing graded dissolution of coccoliths, only a few such studies have been conducted, with a focus on *Gephyrocapsa spp*, in particular *G. huxleyi*, a widely used model species (McIntyre & McIntyre 1971, Burns 1977, Kleijne 1990, Henriksen et al 2004, Langer et al 2006b, Holcová and Scheiner 2023). While *G. huxleyi* is numerically the most abundant coccolithophore in present oceans, its contribution to coccolithophore $CaCO_3$ production is rivalled by some genera with larger coccoliths, such as *Calcidiscus* and *Coccolithus* (Wheeler et al 2023). The relatively recent appearance of *G. huxleyi* in the fossil record implies that this species is not applicable to deep time sediment core studies (Henderiks et al 2022). It is therefore worthwhile also studying genera with larger coccoliths and mass,

https://doi.org/10.5194/egusphere-2025-1921
Preprint. Discussion started: 25 June 2025

biogeographically important ((Ziveri et al., 2004), and with a more extensive evolutionary history, e.g. *Coccolithus*, *Helicosphaera*, and *Scyphosphaera* (Henderiks et al 2022).

Based largely on field sediment studies, it is accepted that some coccolith forms dissolve faster than others. While *G. huxleyi* and *Umbilicosphaera sibogae* are among the fast-dissolving placolith bearing species, *G. oceanica*, *C. leptoporus*, and *C. pelagicus* are comparatively slow-dissolving (McIntyre & McIntyre 1971, Berger 1973, Roth and Coulbourn 1982). These studies have not assessed how dissolution morphologies of different species relate to each other. In other words, which dissolution morphology of species x corresponds to a given dissolution morphology of species y? Knowledge of such differential dissolution morphologies will aid interpretation of field samples, e.g. the degree of dissolution in one species will inform inferences about the degree of dissolution in other species. More fundamentally, knowledge about dissolution morphologies will enable us to accurately distinguish malformation / under-calcification from dissolution, which is not necessarily an easy task (Young 1994). Finally, dissolution might reveal informative structural features, as in the *C. leptoporus* example given above.

In this study we selected laboratory cultures of *Coccolithus braarudii*, *Helicosphaera carteri*, and *Scyphosphaera apsteinii*, and performed a dissolution experiment to follow their differential dissolution morphologies by means of sequential sampling for SEM analysis.

2) Material and Methods

2.1) *Culture conditions*

Clonal cultures of *Coccolithus braarudii* (strain RCC1198), *Scyphosphaera apsteinii* (strain RCC3598), and *Helicosphaera carteri* (strain RCC1323) were grown in aged (3 months), sterile-filtered (Stericup-GP Sterile Vacuum Filtration System, 0.22 µm pore size, polyethersulfone membrane, Merck) natural surface seawater sampled in the English Channel off Roscoff, France, enriched with 288 µM nitrate, 18 µM phosphate, and silicate, trace metals, and vitamins as in K/2-I (https://roscoff-culture-

https://doi.org/10.5194/egusphere-2025-1921
Preprint. Discussion started: 25 June 2025

collection.org/medium-id/k2-i). All strains were obtained from the Roscoff Culture Collection (http://www.roscoff-culture-collection.org).

Cultures were grown under a 16:8 h light:dark cycle at a light intensity of 50 µmol photons m^{-2} s^{-1} in temperature-controlled culture incubators. *Coccolithus braarudii* RCC1198 was grown at 15°C, while *Scyphosphaera apsteinii* RCC3598 and *Helicosphaera carteri* RCC1323 were grown at 20°C. Cells were grown in dilute batch cultures, ensuring a quasi-constant seawater carbonate system over the course of exponential growth (Hoffmann et al. 2015). Cell densities were determined by flow cytometry immediately after sampling. Cultures used in the dissolution experiment were initially checked by light and scanning electron microscopy to ensure that coccosphere morphology was normal (as observed in light microscopy) and the percentage of coccolith malformations was below 15% (as determined by SEM analysis, Langer and Bode 2011). The latter is a very low percentage of malformations in cultures (in which values up to 90% have been reported, Langer et al 2006, Langer et al 2013), enabling this study to focus on normal coccoliths and their dissolution morphologies, as opposed to the dissolution features of malformed coccoliths (Langer and Bode 2011, Langer et al 2013, Langer et al 2023). We chose not to analyse the dissolution morphology of malformed coccoliths because results are intended to be applicable to field samples, in which the percentage of malformed coccoliths is typically only ca. 2% (Langer et al 2006, Langer et al 2013). Analysis of the dissolution morphologies of malformed coccoliths would require a different experimental setup, with cultures displaying high proportions of malformed coccoliths. Such an approach would be interesting in itself, but does not fall within the scope of the present study (Langer et al 2006).

2.2) *Dissolution experiment*

To study differential dissolution morphologies accurately, the selected species have to be exposed to the same seawater, i.e. be present in the same vessel (Holcová and Scheiner 2023), in which case only one calcite saturation state (omega) value can be selected. In pre-experiments we found that *Gephyrocapsa huxleyi* coccoliths dissolved more than 10x faster than coccoliths of *Coccolithus braarudii*, *Helicosphaera carteri*, and *Scyphosphaera apsteinii*, meaning it was not possible to include *G. huxleyi* in our experiment. The three other species, *C. braarudii*, *H. carteri*, and *S. apsteinii*, displayed broadly similar dissolution kinetics and were therefore suited for our purpose.

https://doi.org/10.5194/egusphere-2025-1921
Preprint. Discussion started: 25 June 2025

To start the dissolution experiment, living cells were transferred into a 2.7L bottle containing culture medium that was acidified using calculated amounts of HCl (3.29M) immediately prior to cell transfer. We used acidification to manipulate omega calcite because it is more representative of dissolution scenarios in the field than changes in Ca concentration. This decision is important because the manipulation of omega calcite via acidification is more effective than via Ca concentration decrease (Hassenkam et al 2011). The culture medium prepared using natural surface seawater sampled off Roscoff, France has a typical dissolved inorganic carbon, DIC, of ca 2000 µmol kg^{-1} (Johnson et al 2022). We used this value for DIC and measured pH (NBS) = 6.44 to calculate omega calcite = 0.033 using the program CO2SYS (Pierrot et al 2011). The calculated value for omega calcite (0.033) was therefore approximate. However, DIC variability of natural surface seawater sampled off Roscoff, France is low, therefore introducing only a negligible inaccuracy in calculated omega calcite in the context of the present study, i.e. an error of ±0.005 is expected (Johnson et al 2022). The present study was not designed to analyse dissolution kinetics precisely (such as in Subhas et al 2018), meaning an approximate determination of the carbonate system is sufficient. We used a Cyberscan 500 pH meter equipped with a Mettler Toledo InLab 413/ID67 electrode to determine pH on the NBS scale.

Experimental dissolution over a very short space of time (on the order of seconds as in Yang et al 2021) only allows for comparatively low-resolution light micrographs that would have been insufficient for our purpose. The advantage of a short experiment duration, however, is that DIC uptake and gas exchange with the atmosphere, and therefore carbonate system variability, is negligible. Our dissolution experiment, conducted over a duration of 11 hours, was carried out in the dark at 4°C to ensure that cellular metabolism (including photosynthesis and coccolith production) was severely restricted over the course of the experiment. Cell densities were 711 cells/mL for *C. braarudii*, 665 cells/mL for *H. carteri*, and 586 cells/mL for *S. apsteinii*. The resultant low overall cell density of 1963 cells/mL contributed to ensuring a quasi-constant carbonate system over the course of the experiment (Langer et al 2006, Langer and Bode 2011, Hoffmann et al 2015). Physico-chemical conditions over the course of the experiment were additionally homogenized by regular mixing, i.e. keeping the cells in suspension. No aggregation of cells occurred and no sedimentation of cells or coccoliths took place. The pH did rise by ca 0.1 over the course of the experiment, but this

https://doi.org/10.5194/egusphere-2025-1921
Preprint. Discussion started: 25 June 2025

corresponds to an increase in omega calcite of only ca. 0.005, i.e. the same magnitude as the minor uncertainty introduced by our choice of DIC value (see above).

After the dissolution experiment was completed, cells were transferred into normal culture conditions as specified above. All three species, *C. braarudii*, *H. carteri*, and *S. apsteinii*, resumed cell division and coccolith production as confirmed by optical inspection using light microscopy. We did not quantify coccolith morphology in re-calcifying cells, but noted that initially coccoliths seemed to display more malformations than prior to the dissolution experiment.

Multiple (15) sequential samples for detailed morphological analysis were taken over the 11 hour duration of the experiment. Samples for SEM analysis were filtered onto polycarbonate filters (0.8 µm pore-size), dried in a drying cabinet at 50°C for 24 h, then sputter-coated with gold–palladium using a Cressington 108 sputter coater (Cressington Scientific Instruments, Watford, UK). Imaging was performed with a Phenom Pro desktop SEM at the Station Biologique de Roscoff, France, and an El SEM Zeiss Merlin at UAB, Barcelona, Spain. An average of ~350 coccoliths was analysed per sample (Langer and Benner 2009). To describe dissolution morphologies, we selected conspicuous features that could be easily followed over the course of the experiment to ensure robust results and to facilitate application to field samples. In *C. braarudii* and *H. carteri* we analysed dissolution features of coccospheres in addition to dissolution features of coccoliths. In *S. apsteinii* only dissolution features of coccoliths were analysed because coccospheres in this species lack the mechanical stability needed to consistently withstand the mechanical forces experienced in SEM preparation (Langer et al 2023). The following morphological features were used to describe dissolution. In *C. braarudii*: 1) etching of the inner tube, 2) etching of the distal shield, 3) central area bar missing, 4) coccoliths broken, 5) gaps in coccospheres, 6) coccospheres collapsed, 7) nanostructure visible (on proximal side of distal shield). In *H. carteri*: 1) etching, 2) coccoliths broken, 3) coccospheres collapsed. In *S. apsteinii* lopadoliths: 1) etching of base, 2) etching of barrel, 3) rim serrated, 4) lopadoliths broken, 5) isolated lopadolith V units. In *S. apsteinii* muroliths: 1) centre missing, 2) etching, 3) muroliths broken. Scanning electron micrographs of all of these features are shown in Figs 1-5.

3) Results and Discussion

https://doi.org/10.5194/egusphere-2025-1921
Preprint. Discussion started: 25 June 2025

3.1) Differential dissolution: general observations

We subjected living cells of three common coccolithophore species, namely *Coccolithus braarudii*, *Helicosphaera carteri*, and *Scyphosphaera apsteinii*, to seawater undersaturated with respect to calcite, i.e. omega calcite ca. 0.033 (see Methods). The duration of the experiment was 11 hours, at the end of which only a few isolated distal shield elements of *C. braarudii* remained (Fig 6). Our observation that *C. braarudii* is more dissolution resistant than *H. carteri* tallies well with conclusions drawn from studying Atlantic Ocean floor sediments (Berger 1973). Information on *S. apsteinii* in differential dissolution studies is rare, with this species either only mentioned but not discussed or not mentioned at all (McIntyre & McIntyre 1971, Berger 1973, Roth and Coulbourn 1982). From our data we conclude that *S. apsteinii* lopadoliths display dissolution kinetics similar to *H. carteri*, while *S. apsteinii* muroliths dissolve faster. *S. apsteinii* lopadolith R-units conspicuously dissolve faster than V-units (Figs 6, 7), potentially as a result of the size difference of the individual crystals, with V-units being larger (see also Drescher et al 2012). The different dissolution kinetics of V and R units in the same lopadolith illustrates that the microstructure of a $CaCO_3$ biomineral influences dissolution kinetics, which could not be inferred from its polymorph alone (the only polymorph that lopadoliths contain is calcite; Walker et al 2024, Langer and Ziveri, in press). Both etching and broken coccoliths appear simultaneously in *S. apsteinii* lopadoliths and *H. carteri* (Figs 6, 7). In *C. braarudii* etching of the inner tube occurs simultaneously with etching in *H. carteri* and *S. apsteinii*, but etching of the *C. braarudii* distal shield appears later, possibly because the latter features the largest crystals (Figs 6, 7). Relatively slow dissolution of the distal shield compared to the tube/central area was also observed in *C. leptoporus* and might be a general feature of Coccolithales placoliths (Langer et al 2007).

3.2) Comparison with field samples

As noted in the introduction coccolith dissolution in the water column is being highlighted as a key process, greatly affecting the export production of coccolith $CaCO_3$ to the bottom sediment. Our experimental results on the sequence of dissolution stages might usefully be applied to study of field samples in order to analyse and track water column dissolution. As a proof of concept we show here (Fig 8) images of *Coccolithus braarudii* and *Helicosphaera carteri* coccoliths from sediment trap samples and of coccoliths from water column samples, in both cases showing dissolution features

https://doi.org/10.5194/egusphere-2025-1921
Preprint. Discussion started: 25 June 2025

directly comparable to those we observed experimentally. It is also noteworthy that the nanostructure seen in the experimental samples is visible in the field samples (Fig 8) showing that it is not an experimental artefact. Comparable dissolution features have also been illustrated in the literature, for example by Cubillos et al (2012) and Kleijne (1990), although in some cases they have been ascribed to malformation.

As a caveat we will say that dissolution morphologies might well depend on the conditions under which dissolution occurs. For example, the presence or absence of an organic coating around coccoliths results in slightly different dissolution morphologies as seen in high resolution AFM imaging (Henriksen et al 2004). Since we did not remove the organic coating, our results should be best applicable to water samples (with organic coating) as opposed to sediment samples (in which the organic coating might be degraded). That said, the organic coating of coccoliths can still slow down dissolution after 70Ma in the sediment (Sand et al 2014). Whether dissolution morphologies of these ancient coccoliths would be similar to those of cultured specimens remains to be tested. A good candidate would be *C. pelagicus* because it first appeared in the fossil record more than 60 Ma (Henderiks et al 2022). Another aspect to consider is the way undersaturation is achieved. Dissolution kinetics in low-Ca solutions are different from those in low-pH solutions (Hassenkam et al 2011). It is an open question whether dissolution morphologies would differ too. In addition, pressure-driven undersaturation might be relevant for deep-sea sediment samples. All of these issues are amenable to experimental testing and should be the focus of future studies.

3.3) Structural integrity of the coccosphere

An interesting difference between *C. leptoporus* (Langer et al 2007) on the one hand and *C. braarudii / H. carteri* (this study) on the other hand is the structural integrity of coccospheres under dissolution. The earliest feature of dissolution in *C. leptoporus* is the separation of the shields resulting in coccosphere collapse (Langer et al 2007). By contrast, in *C. braarudii* and *H. carteri* the earliest dissolution feature is etching leaving the coccospheres intact. Only when coccoliths break due to more pronounced etching do coccospheres collapse in these species (Fig 7). This means that living *C. leptoporus* cells are more vulnerable to dissolution than *C. braarudii / H. carteri* because all three species need a coccosphere to live (Walker et al 2018a, Bianco et al., 2025). This vulnerability sequence differs from what would be expected based on species specific coccolith solubility as inferred from sediment samples, which do not

https://doi.org/10.5194/egusphere-2025-1921
Preprint. Discussion started: 25 June 2025

suggest that *C. leptoporus* is more vulnerable than *H. carteri* (Berger 1973). Note that we cannot be entirely sure that *C. leptoporus* coccoliths would break faster than *H. carteri* coccoliths when subjected to the same omega calcite because the *C. leptoporus* experiment was conducted at an omega calcite of 0.5 (Langer et al 2007) as opposed to the ca 0.033 used here. Nevertheless, considering the very early appearance of separated shields in *C. leptoporus* (Langer et al 2007) and the comparatively late appearance of broken coccoliths in *H. carteri*, it is highly likely that coccosphere collapse in *C. leptoporus* would occur earlier than in *H. carteri* (at a given omega calcite).

3.4) *A nanostructure in C. braarudii biomineral*

A nanostructure on the proximal side of the distal shield in *C. braarudii* became visible 3 hours into the experiment (Fig. 6). The individual "units" of this nanostructure are ca. 50-100 nm in diameter. The distal side of the distal shield does not show this nanostructure. Differences between the proximal and distal sides of the distal shield have previously been reported (Henriksen et al 2004, Young et al 2004). Whereas the distal side of the distal shield consists of crystallographic a-faces, the proximal side seems to be more profoundly regulated by the cell and does not show crystallographic faces (Young et al 2004). The nanostructure shown here is what was described as "tuberculate surface" by Henriksen et al. (2004). The latter authors conclude that the tubercles are part of the calcite structure. We confirm this conclusion which is illustrated particularly well by a side view of these tubercles (Fig. 3D). A nanostructure of similar size in $CaCO_3$ biominerals is widespread in extracellular calcifiers, where it is a central indicator of a layered growth mechanism featuring particle accretion which is believed to be non-operative in coccolithophores (Kadan et al 2021, Walker and Langer 2021). It remains, however, an open question whether the nanostructure in *C. braarudii* is similar to that in extracellular calcifiers i.e. whether it is also an organo-mineral composite structure (Walker and Langer 2021). This question is pertinent to coccolithophore biomineralization because an extracellular-like nanostructure in coccoliths would call into question widely held views about crystallization of coccolith crystals (Walker and Langer 2021). However, even if the tuberculate nanostructure in *C. braarudii* should turn out to be extracellular-like, it would still be unclear how it is possible that the distal side of the distal shield is different, i.e. shows crystallographic a-faces and no nanostructure. The standard biomineralization model explaining the nanostructure in extracellular calcifiers cannot account for the difference between the two sides of the

https://doi.org/10.5194/egusphere-2025-1921
Preprint. Discussion started: 25 June 2025

distal shield in *C. braarudii*, and neither can the standard model of coccolith biomineralization (Young et al 2004, Walker and Langer 2021). This difference between the proximal and the distal side of the distal shield shows how finely tuned morphogenesis in *C. braarudii* is. We can only speculate how this fine tuning is achieved, but the composition of the organic coating might play a role. The composition of coccolith associated polysaccharides is known to be species specific, but we speculate that it might also be site specific within the coccolith vesicle (Walker et al 2018b).

4) Conclusions

In summary, our results show that dissolution experiments complement field studies and contribute to a deeper understanding of both coccolith structure and the ecological impact of seawater undersaturation with respect to calcite. We conclude that

1) the most dissolution-resistant species is *C. braarudii*, followed by *H. carteri* and *S. apsteinii*;

2) structural integrity of the coccosphere under dissolution is highest in *C. braarudii*, followed by *H. carteri* and *S. apsteinii*, with *C. leptoporus* probably showing the weakest coccosphere;

3) we identify dissolution in published field data where it was not recognised;

4) lopadolith R-units dissolve faster than V-units, illustrating that different microstructures in the same coccolith have different dissolution kinetics despite containing the same mineral;

5) the nanostructure in the distal shield of *C. braarudii* points to a fine-tuning in coccolith morphogenesis that is not accounted for by our current model of coccolith biomineralization.

Acknowledgements

No acknowledgements at this stage.

Funding:

https://doi.org/10.5194/egusphere-2025-1921
Preprint. Discussion started: 25 June 2025

Generalitat de Catalunya (MERS, 2021 SGR00640), Spanish Ministry of Science and Innovation (CEX2019-000940-M), and BIOCAL project (PID2020-113526RB-I00, Spanish Ministry of Science and Innovation).

Competing interests

The authors declare no conflict of interests.

Author contributions

GL: conception, experiments, analysis, writing, IP: experiments, writing, JRY: analysis, field samples, writing, PZ: writing.

Data availability

Data will be made available at Pangaea database.

References

Berger WH (1973) Deep-sea carbonates: evidence for a coccolith lysocline. Deep-Sea Res 20:917–921

Bianco, S., Bordiga, M., Langer, G., Ziveri, P., Cerino, F., Di Giulio, A., and Lupi, C. (2025) Low sensitivity of a heavily calcified coccolithophore under increasing CO2: the case study of Helicosphaera carteri, Biogeosciences, 22, 1821–1837, https://doi.org/10.5194/bg-22-1821-2025.

Broecker, W. & Clark, E. Ratio of coccolith CaCO3 to foraminifera CaCO3 in late Holocene deep sea sediments. Paleoceanogr. 24, PA3205 (2009).

Broecker, W. S. & Peng, T.-H. Tracers in the Sea. 690 (Lamont-Doherty Geological Observatory, Columbia University, 1982)

Broerse, A.T.C., Ziveri, P., Honjo, S., (2000) Coccolithophore (CaCO3) flux in the Sea of Okhotsk: seasonality, settling and alteration processes Marine Micropaleontology, 39 (1-4): 179-200.

Burns, D. A. (1977). Phenotypes and dissolution morphotypes of the genus Gephyrocapsa Kamptner and Emiliania huxleyi (Lohmann). New Zealand Journal of Geology and Geophysics, 20(1), 143-155.

https://doi.org/10.5194/egusphere-2025-1921
Preprint. Discussion started: 25 June 2025

Cubillos, J.C., Henderiks, J., Beaufort, L., Howard, W.R., & Hallegraeff, G.M. (2012). Reconstructing calcification in ancient coccolithophores: Individual coccolith weight and morphology of Coccolithus pelagicus (sensu lato). Marine Micropaleontology, 92, 29-39.

Drescher B, Dillaman RM, Taylor AR. (2012) Coccolithogenesis In Scyphosphaera apsteinii (Prymnesiophyceae). J Phycol. 2012 Dec;48(6):1343-61. doi: 10.1111/j.1529-8817.2012.01227.x. Epub 2012 Sep 17. PMID: 27009987.

Guptha, .M., Banerjee, R. & Mergulhao, L. On the nature of the calcareous substrate of a ferromanganese crust from the Vityaz Fracture Zone, Central Indian Ridge: (2002). inferences on paleoceanography. Geo-Mar Lett 22, 12–18 (2002). https://doi.org/10.1007/s00367-002-0091-0

Hassenkam, T., Johnsson, A. M. S., Bechgaard, K., & Stipp, S. L. S. (2011). Tracking single coccolith dissolution with picogram resolution and implications for CO2 sequestration and ocean acidification. Proceedings of the National Academy of Sciences of the United States of America, 108, 8571-8576.

Henderiks, J., Sturm, D., Šupraha, L., & Langer, G. (2022). Evolutionary Rates in the Haptophyta: Exploring Molecular and Phenotypic Diversity. Journal of Marine Science and Engineering, 10(6), 798. https://doi.org/10.3390/jmse10060798

Henriksen, K., Young, J. R., Bown, P. R., & Stipp, S. L. S. (2004). Coccolith biomineralisation studied with atomic force microscopy. Palaeontology, 47(3), 725-743.

Hoffmann, R., Kirchlechner, C., Langer, G., Wochnik, A. S., Griesshaber, E., Schmahl, W. W., and Scheu, C. (2015) Insight into Emiliania huxleyi coccospheres by focused ion beam sectioning, Biogeosciences, 12, 825–834, https://doi.org/10.5194/bg-12-825-2015, 2015.

Holcová K, Scheiner F. (2023). An experimental study on post-mortem dissolution and overgrowth processes affecting coccolith assemblages: A rapid and complex process. Geobiology. 2023 Mar;21(2):193-209. doi: 10.1111/gbi.12528. Epub 2022 Oct 11. PMID: 36218003.

Honjo,S. 1975. "DISSOLUTION OF SUSPENDED COCCOLITHS IN THE DEEP-SEA WATER COLUMN AND SEDIMENTATION OF COCCOLITH OOZE",

https://doi.org/10.5194/egusphere-2025-1921
Preprint. Discussion started: 25 June 2025

Dissolution of Deep-sea Carbonates, William V. Sliter, Allan W. H. Bé, Wolfgang H. Berger

Johnson, R., Langer, G., Rossi, S., Probert, I., Mammone, M., & Ziveri, P. (2022). Nutritional response of a coccolithophore to changing pH and temperature. Limnology and Oceanography, 67(10), 2309-2324.

Kadan Y, Tollervey F, Varsano N, Mahamid J, Gal A. (2021) Intracellular nanoscale architecture as a master regulator of calcium carbonate crystallization in marine microalgae. Proc Natl Acad Sci U S A. 2021 Nov 16;118(46):e2025670118. doi: 10.1073/pnas.2025670118. PMID: 34772804; PMCID: PMC8694050.

Kleijne, A. (1990). Distribution and malformation of extant calcareous nannoplankton in the Indonesian Seas. Marine Micropaleontology, 16(3-4), 293-316.

Langer, G. & Benner, I. (2009) Effect of elevated nitrate concentration on calcification in Emiliania huxleyi. J. Nannoplankton Res. 30: 77–80.

Langer, G., & Bode, M. (2011). CO2 mediation of adverse effects of seawater acidification in Calcidiscus leptoporus. Geochemistry, Geophysics, Geosystems, 12(5). https://doi.org/10.1029/2010GC003393

Langer, G., Geisen, M., Baumann, K. H., Kläs, J., Riebesell, U., Thoms, S., & Young, J. R. (2006). Species-specific responses of calcifying algae to changing seawater carbonate chemistry. Geochemistry, geophysics, geosystems, 7(9).

Langer, G., Gussone, N., Nehrke, G., Riebesell, U., Eisenhauer, A., Kuhnert, H., Rost, B., Trimborn, S., & Thoms, S. (2006b). Coccolith strontium to calcium ratios in Emiliania huxleyi: The dependence on seawater strontium and calcium concentrations. Limnology and Oceanography, 51(1 I), 310-320. https://doi.org/10.4319/lo.2006.51.1.0310

Langer, G., Nehrke, G., & Jansen, S. (2007). Dissolution of Calcidiscus leptoporus coccoliths in copepod guts? A morphological study. Marine Ecology Progress Series, 331, 139-146.

Langer, G., Oetjen, K., Brenneis, T. (2013). On culture artefacts in coccolith morphology. Helgoland Marine Research, 67(2), 359-369. https://doi.org/10.1007/s10152-012-0328-x

https://doi.org/10.5194/egusphere-2025-1921
Preprint. Discussion started: 25 June 2025

Langer G, Probert I, Cox MB, Taylor A, Harper GM, Brownlee C, Wheeler G. (2023) The Effect of cytoskeleton inhibitors on coccolith morphology in Coccolithus braarudii and Scyphosphaera apsteinii. J Phycol. 2023 Feb;59(1):87-96. doi: 10.1111/jpy.13303. Epub 2022 Dec 24. PMID: 36380706.

Matsuoka, H. (1990) A new method to evaluate dissolution of CaCO3 in the deep-sea sediments. Trans. Proc. Paleont. Soc. Jpn., 157, 430-434

McIntyre A, McIntyre R (1971) Coccolith concentration and differential solution in oceanic sediments. In: Funnel BM, Riedel WR (eds) The micropaleontology of oceans. Cambridge University Press, Cambridge, p 253–261O

Milliman, J. D. Production and accumulation of calcium carbonate in the ocean: budget of a nonsteady state. Glob. Biogeochemical Cycles 7, 927–957 (1993).

Morse, J. W. & Mackenzie, F. T. Geochemistry of sedimentary carbonates. (Elsevier, 1990).

Pierrot, D., D. Wallace, E. Lewis, R. Wallace, and W. Wallace. (2011) MS Excel Program Developed for CO2 System Calculations. ORNL Environmental Sciences Division. doi:10.3334/CDIAC/otg

Roth PH, Berger WH (1975) Distribution and dissolution of coccoliths in the south and central Pacific. In: Sliter WV, Be AWH, Berger WH (eds) CaCO3 dissolution in the deep sea. Cushman Foundation for Foraminiferal Research, Santa Barbara, CA, p 87–113

Roth, P. H., & Coulbourn, W. T. (1982). Floral and solution patterns of coccoliths in surface sediments of the North Pacific. Marine Micropaleontology, 7(1), 1–52. doi:10.1016/0377-8398(82)90014-7

Sand, K., Pedersen, C., Sjoberg, S., Nielsen, J., Makovicky, E., and Stipp, S. (2014). Biomineralization: long-term effectiveness of polysaccharides on the growth and dissolution of calcite. Cryst. Growth Des. 14, 5486–5494. doi: 10.1021/cg5006743

Subhas, A. V., Rollins, N. E., Berelson, W. M., Erez, J., Ziveri, P., Langer, G., & Adkins, J. F. (2018). The dissolution behavior of biogenic calcites in seawater and a possible role for magnesium and organic carbon. Marine Chemistry, 205, 100-112. https://doi.org/10.1016/j.marchem.2018.08.001

https://doi.org/10.5194/egusphere-2025-1921
Preprint. Discussion started: 25 June 2025

464 Subhas, A. V., Dong, S., Naviaux, J. D., Rollins, N. E., Ziveri, P., Gray, W., Rae, J. W.
465 B., Liu, X., Byrne, R. H., Chen, S., Moore, C., Martell-Bonet, L., Steiner, Z., Antler, G.,
466 Hu, H., Lunstrum, A., Hou, Y., Kemnitz, N., Stutsman, J., … Adkins, J. F. (2022).
467 Shallow Calcium Carbonate Cycling in the North Pacific Ocean. Global
468 Biogeochemical Cycles, 36(5). https://doi.org/10.1029/2022GB007388

469 Sulpis, O., Jeansson, E., Dinauer, A., Lauvset, S. K., & Middelburg, J. J. (2021).
470 Calcium carbonate dissolution patterns in the ocean. Nature Geoscience, 14(6), 423–
471 428. https://doi.org/10.1038/s41561-021-00743-y

472 Walker JM, Langer G. (2021) Coccolith crystals: Pure calcite or organic-mineral
473 composite structures? Acta Biomater. 2021 Apr 15;125:83-89. doi:
474 10.1016/j.actbio.2021.02.025. Epub 2021 Feb 22. PMID: 33631395.

475 Walker JM, Greene HJM, Moazzam Y, Quinn PD, Parker JE, Langer G. (2024) An
476 uneven distribution of strontium in the coccolithophore Scyphosphaera apsteinii
477 revealed by nanoscale X-ray fluorescence tomography. Environ Sci Process Impacts.
478 2024 Jun 19;26(6):966-974. doi: 10.1039/d3em00509g. PMID: 38354057.

479 Walker CE, Taylor AR, Langer G, Durak GM, Heath S, Probert I, Tyrrell T, Brownlee
480 C, Wheeler GL. (2018a) The requirement for calcification differs between ecologically
481 important coccolithophore species. New Phytol. 2018 Oct;220(1):147-162. doi:
482 10.1111/nph.15272. Epub 2018 Jun 19. PMID: 29916209; PMCID: PMC6175242.

483 Walker, Charlotte E., Heath, Sarah, Salmon, Deborah L., Smirnoff, Nicholas, Langer,
484 Gerald, Taylor, Alison R., Brownlee, Colin and Wheeler, Glen L. (2018b) An
485 extracellular polysaccharide-rich organic layer contributes to organization of the
486 coccosphere in coccolithophores. Frontiers in Marine Science, 5 (AUG), [306].
487 (doi:10.3389/fmars.2018.00306).

488 Wheeler GL, Sturm D, Langer G. (2023) Gephyrocapsa huxleyi (Emiliania huxleyi) as a
489 model system for coccolithophore biology. J Phycol. 2023 Dec;59(6):1123-1129. doi:
490 10.1111/jpy.13404. Epub 2023 Nov 20. PMID: 37983837.

491 Yang M, Batchelor-McAuley C, Barton S, Rickaby REM, Bouman HA, Compton RG.
492 (2021) Opto-Electrochemical Dissolution Reveals Coccolith Calcium Carbonate
493 Content. Angew Chem Int Ed Engl. 2021 Sep 13;60(38):20999-21006. doi:

https://doi.org/10.5194/egusphere-2025-1921
Preprint. Discussion started: 25 June 2025

10.1002/anie.202108435. Epub 2021 Aug 15. PMID: 34288323; PMCID: PMC8518593.

Young, J. R. (1994). Variation in *Emiliania huxleyi* coccolith morphology in samples from the Norwegian EHUX experiment, 1992. Sarsia. 79(4): 417-425.

Young, J. R. (2008). Scyphosphaera porosa Kamptner 1967 rediscovered in the plankton. Journal of Nannoplankton Research. 30(1): 35-38

Young, J. R., Henriksen, K., & Probert, I. (2004). Structure and morphogenesis of the coccoliths of the CODENET species. In Coccolithophores: From molecular processes to global impact, Thierstein, H. R., & Young, J. R. (Eds.), Springer, 191-216.

Ziveri, P., Baumann, K.H., Böckel, B. Bollmann, J. and Young, J. (2004) Present day coccolithophore-biogeography in the Atlantic Ocean in Thierstein, H. and Young, J. Eds. Coccolithophores: From Molecular Processes to Global Impact. Springer Verlag: 403-428.

Ziveri, P., Gray, W. R., Anglada-Ortiz, G., Manno, C., Grelaud, M., Incarbona, A., Rae, J. W. B., Subhas, A. V., Pallacks, S., White, A., Adkins, J. F., & Berelson, W. (2023). Pelagic calcium carbonate production and shallow dissolution in the North Pacific Ocean. Nature Communications, 14(1), 805. https://doi.org/10.1038/s41467-023-36177-w

Ziveri, P., Passaro, M., Incarbona, A., Milazzo, M., Rodolfo-Metalpa, R., & Hall-Spencer, J. M. (2014). Decline in Coccolithophore Diversity and Impact on Coccolith Morphogenesis Along a Natural CO 2 Gradient. The Biological Bulletin, 226(3), 282–290. https://doi.org/10.1086/BBLv226n3p282

Figure captions

Fig 1 *Coccolithus braarudii*

A) coccosphere at t0, no dissolution B) coccosphere; etching of tube and distal shield and central area bar missing C) broken coccoliths, etching of tube, central bar missing and gaps in coccosphere D) collapsed coccosphere, also showing etching of tube and distal shield and central area bar missing E) coccolith, etching of tube and distal shield,

https://doi.org/10.5194/egusphere-2025-1921
Preprint. Discussion started: 25 June 2025

and central area missing. Note that the etching consistently occurs by opening of sutures between elements rather than by dissolution of element surfaces.

Fig 2 *Coccolithus braarudii*

A) broken coccolith distal shield in distal view. B) broken coccolith proximal view of distal shield showing nanostructure; the arrow indicates isolated distal shield elements in distal view, from another coccolith, not displaying nanostructure on distal and vertical surfaces.

Fig 3 *Coccolithus braarudii*

A) broken coccolith distal shield in proximal view showing nanostructure B) proximal view of distal shield elements showing nanostructure C) proximal view of distal shield elements showing nanostructure; individual "tubercles" of the nanostructure are ca 50-100nm D) isolated distal shield elements showing nanostructure "tubercles" in vertical side view (arrow)

Fig 4 *Helicosphaera carteri*

A) coccosphere at t0, no dissolution B) coccosphere displaying coccoliths with severe etching and a broken coccolith C) collapsed coccosphere including broken coccoliths D) coccoliths in distal view with etching in flange and blanket E) coccolith in distal view with etching in flange and blanket F) coccolith in proximal view with etching in flange

Fig 5 *Scyphosphaera apsteinii*

A) coccosphere at t0, no dissolution B) lopadolith base etching (left); murolith centre missing (right) C) lopadolith barrel etching and serrated rim D and E) broken lopadoliths F) isolated V-units G) murolith at t0, no dissolution H) murolith with etching I) lopadolith in distal view showing R- and V-units (arrows, Young 2008); and broken murolith (right)

https://doi.org/10.5194/egusphere-2025-1921
Preprint. Discussion started: 25 June 2025

552 Fig 6 Timelines of dissolution. Bars indicate the period during which the respective
553 feature can be observed. For example-images of each feature see Figs 1-5.

554

555 Fig 7 Quantification of the observations illustrated in Fig 6. Plotted is the percentage of
556 each analysed feature versus time in hours from start of experiment. A) *Scyphosphaera*
557 *apsteinii* lopadoliths B) *Scyphosphaera apsteinii* muroliths C) *Helicosphaera carteri* D)
558 *Coccolithus braarudii*

559

560 Fig 8 Field samples showing etching patterns comparable to those seen in the
561 experimental samples. All scale bars 2 µm.

562 *Coccolithus braarudii*: A) Lower surface of a broken piece of distal shield showing
563 nanostructure. B) Central area of distal shield showing early stage dissolution. C) Proximal
564 surface showing advanced dissolution.

565 *Helicosphaera carteri*: D) Distal Surface showing early stage dissolution. E) Proximal surface
566 showing advanced dissolution.

567

https://doi.org/10.5194/egusphere-2025-1921
Preprint. Discussion started: 25 June 2025

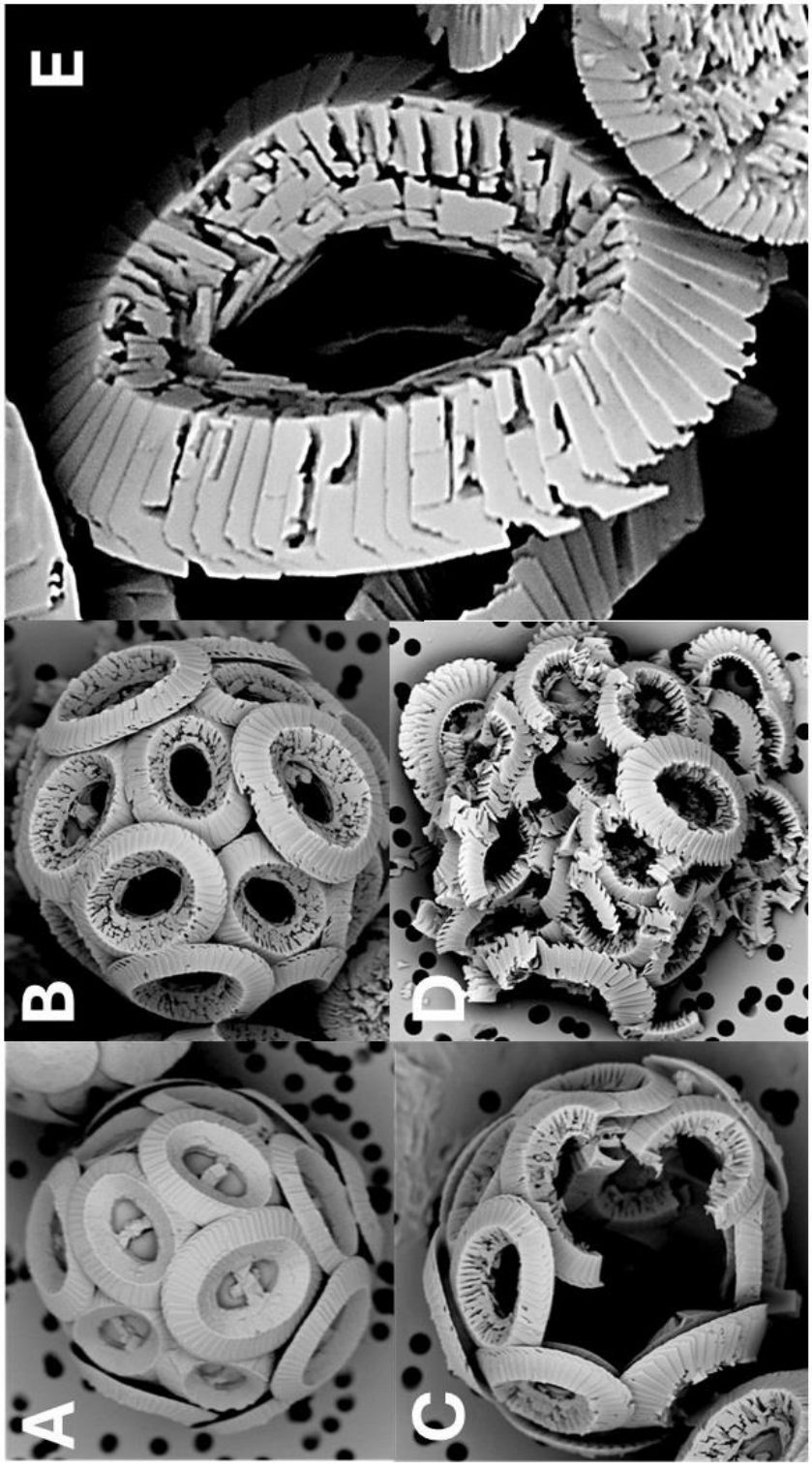

568

https://doi.org/10.5194/egusphere-2025-1921
Preprint. Discussion started: 25 June 2025

Fig 1 *Coccolithus braarudii*

A) coccosphere at t0, no dissolution B) coccosphere; etching of tube and distal shield and central area bar missing C) broken coccoliths, etching of tube, central bar missing and gaps in coccosphere D) collapsed coccosphere, also showing etching of tube and distal shield and central area bar missing E) coccolith, etching of tube and distal shield, and central area missing. Note that the etching consistently occurs by opening of sutures between elements rather than by dissolution of element surfaces.

https://doi.org/10.5194/egusphere-2025-1921
Preprint. Discussion started: 25 June 2025

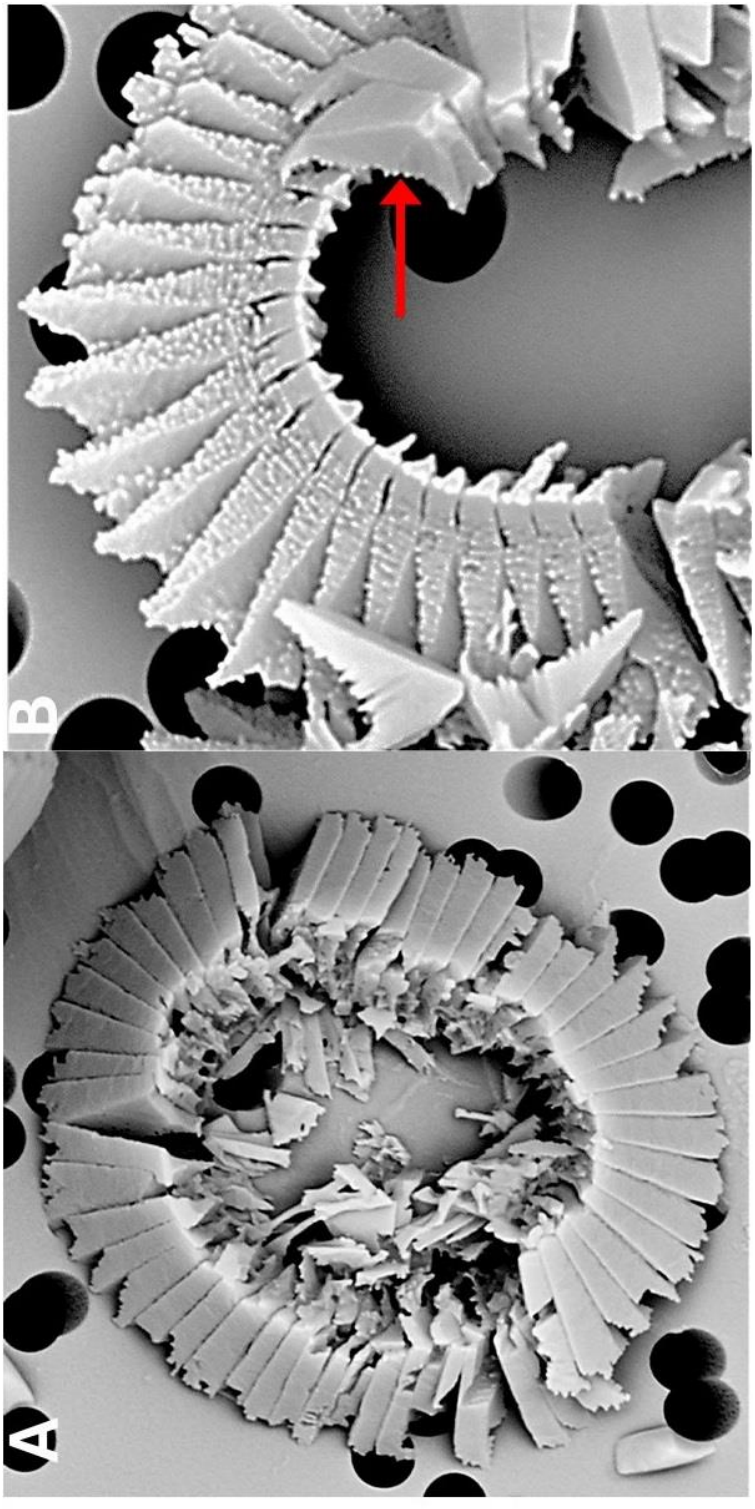

577

https://doi.org/10.5194/egusphere-2025-1921
Preprint. Discussion started: 25 June 2025

Fig 2 *Coccolithus braarudii*

A) broken coccolith distal shield in distal view. B) broken coccolith proximal view of distal shield showing nanostructure; the arrow indicates isolated distal shield elements in distal view, from another coccolith, not displaying nanostructure on distal and vertical surfaces.

https://doi.org/10.5194/egusphere-2025-1921
Preprint. Discussion started: 25 June 2025

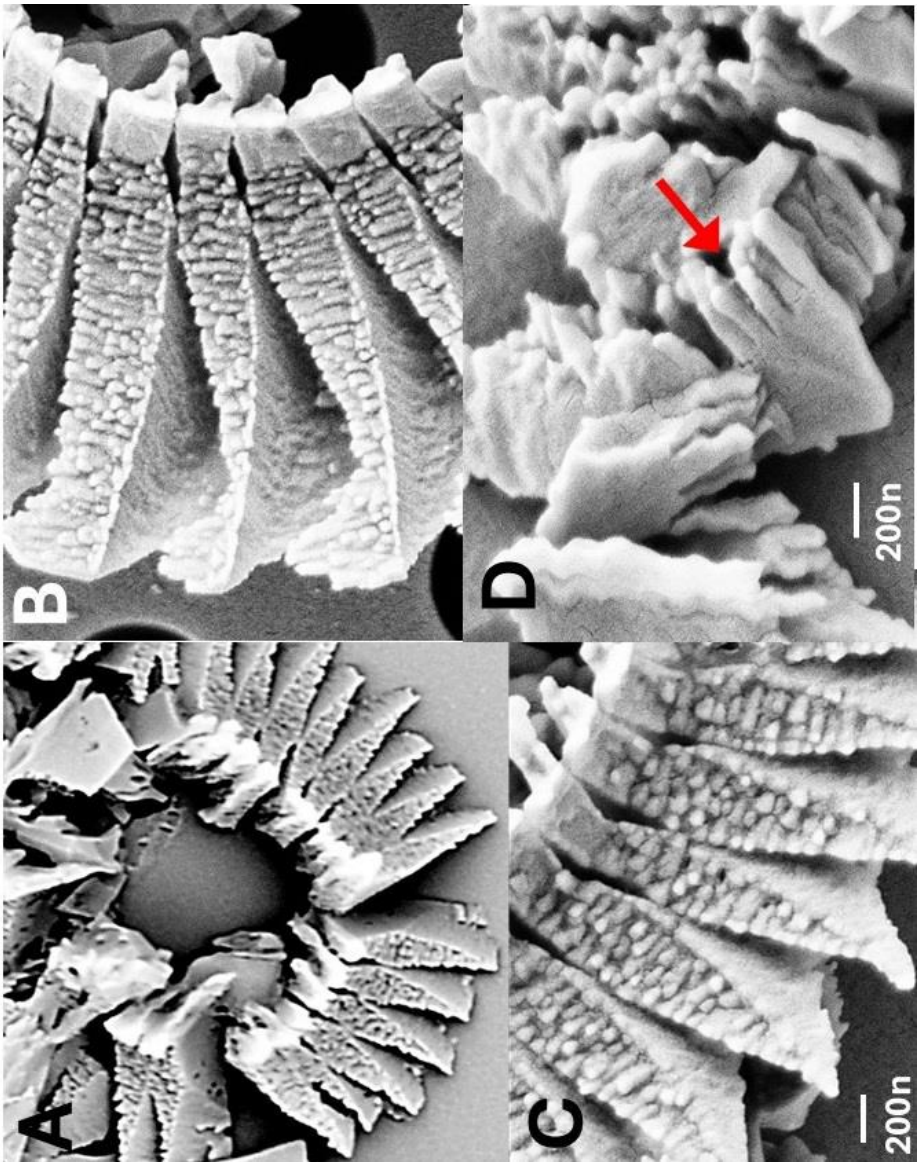

585

https://doi.org/10.5194/egusphere-2025-1921
Preprint. Discussion started: 25 June 2025

586 Fig 3 *Coccolithus braarudii*

587 A) broken coccolith distal shield in proximal view showing nanostructure B) proximal
588 view of distal shield elements showing nanostructure C) proximal view of distal shield
589 elements showing nanostructure; individual "tubercles" of the nanostructure are ca 50-
590 100nm D) isolated distal shield elements showing nanostructure "tubercles" in vertical
591 side view (arrow)

592

593

https://doi.org/10.5194/egusphere-2025-1921
Preprint. Discussion started: 25 June 2025

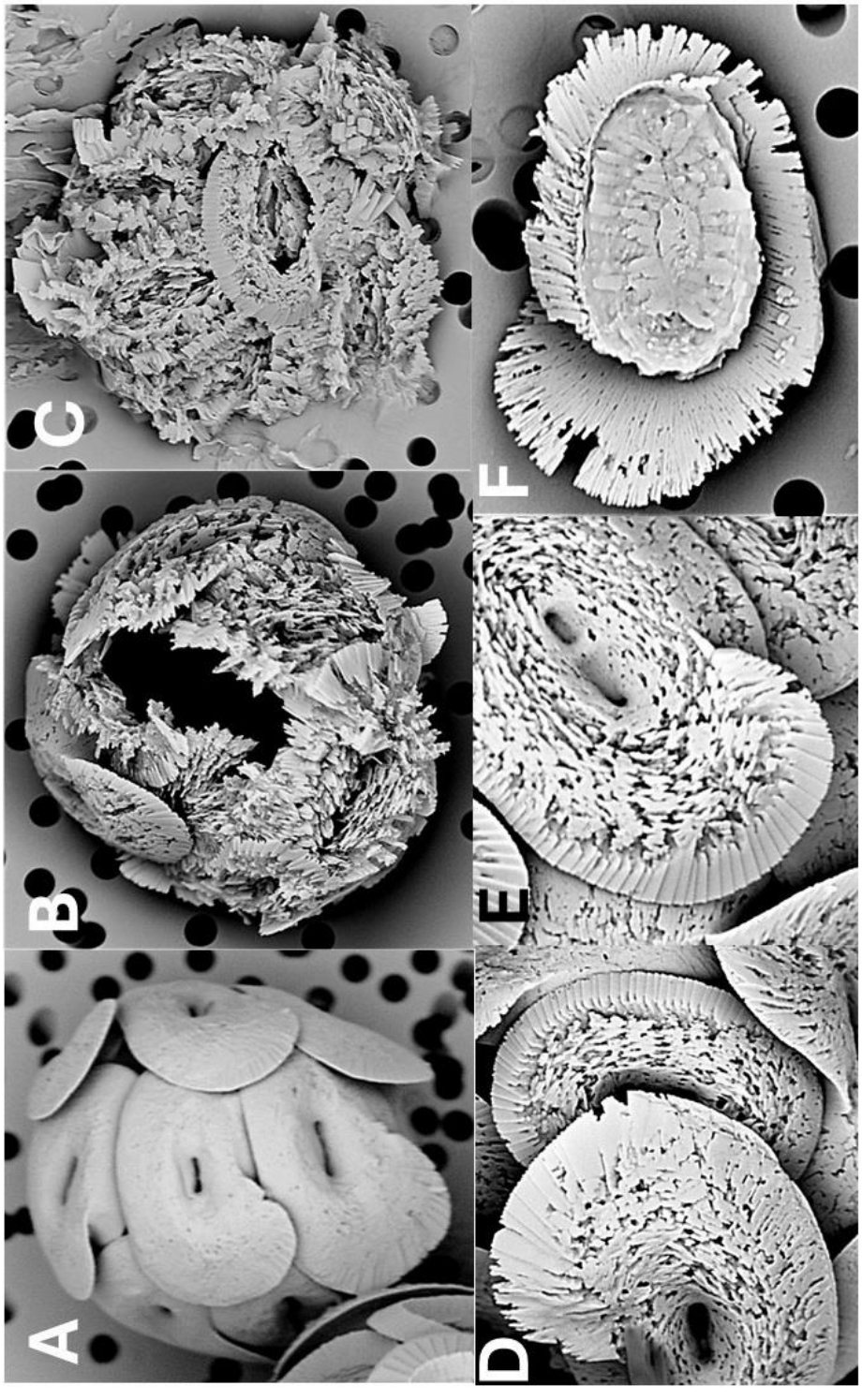

https://doi.org/10.5194/egusphere-2025-1921
Preprint. Discussion started: 25 June 2025

595 Fig 4 *Helicosphaera carteri*

596 A) coccosphere at t0, no dissolution B) coccosphere displaying coccoliths with severe
597 etching and a broken coccolith C) collapsed coccosphere including broken coccoliths D)
598 coccoliths in distal view with etching in flange and blanket E) coccolith in distal view
599 with etching in flange and blanket F) coccolith in proximal view with etching in flange

600

601

https://doi.org/10.5194/egusphere-2025-1921
Preprint. Discussion started: 25 June 2025

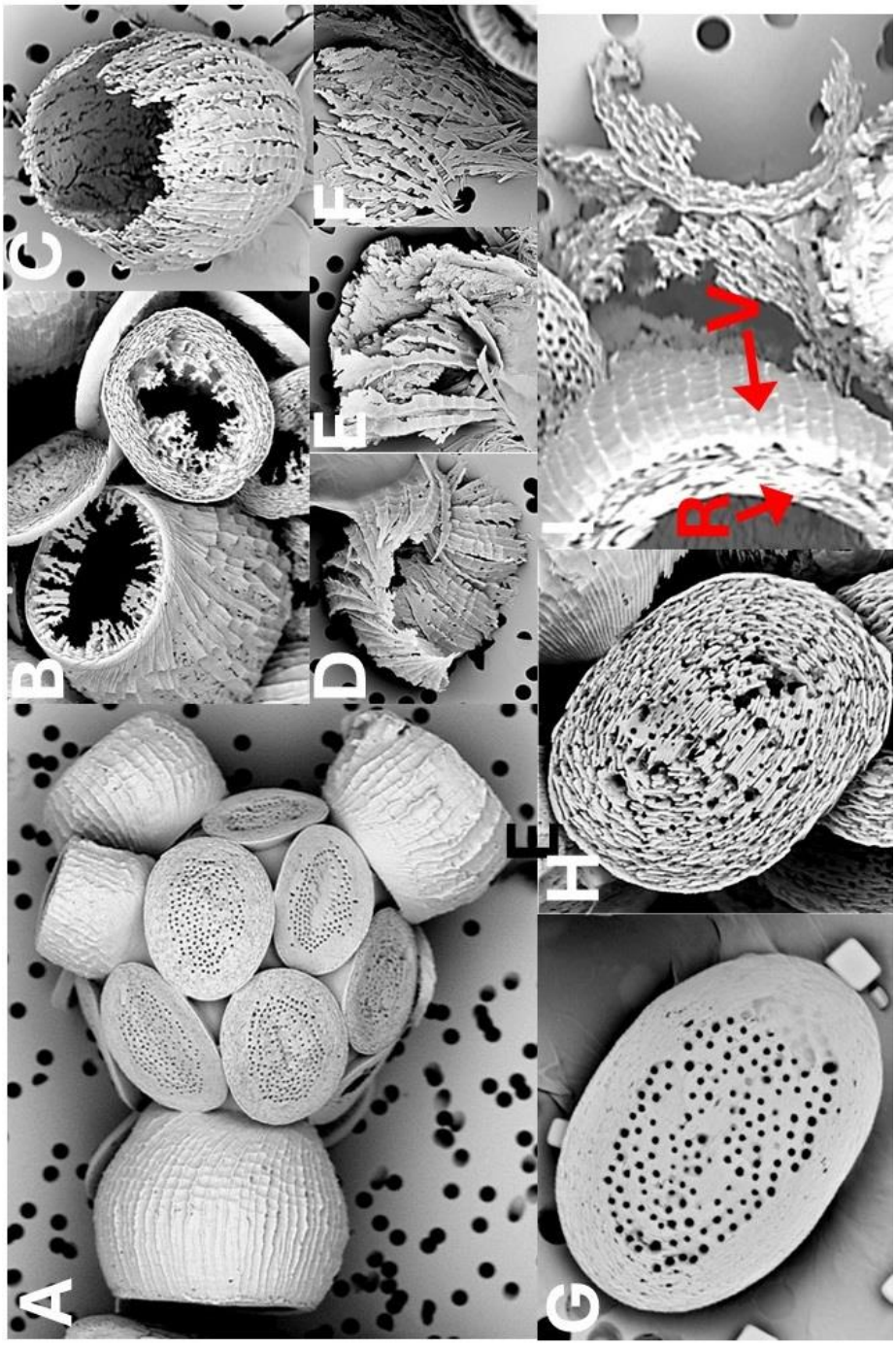

602

https://doi.org/10.5194/egusphere-2025-1921
Preprint. Discussion started: 25 June 2025

603 Fig 5 *Scyphosphaera apsteinii*

604 A) coccosphere at t0, no dissolution B) lopadolith base etching (left); murolith centre
605 missing (right) C) lopadolith barrel etching and serrated rim D and E) broken
606 lopadoliths F) isolated V-units G) murolith at t0, no dissolution H) murolith with
607 etching I) lopadolith in distal view showing R- and V-units (arrows, Young 2008); and
608 broken murolith (right)

609

610

https://doi.org/10.5194/egusphere-2025-1921
Preprint. Discussion started: 25 June 2025

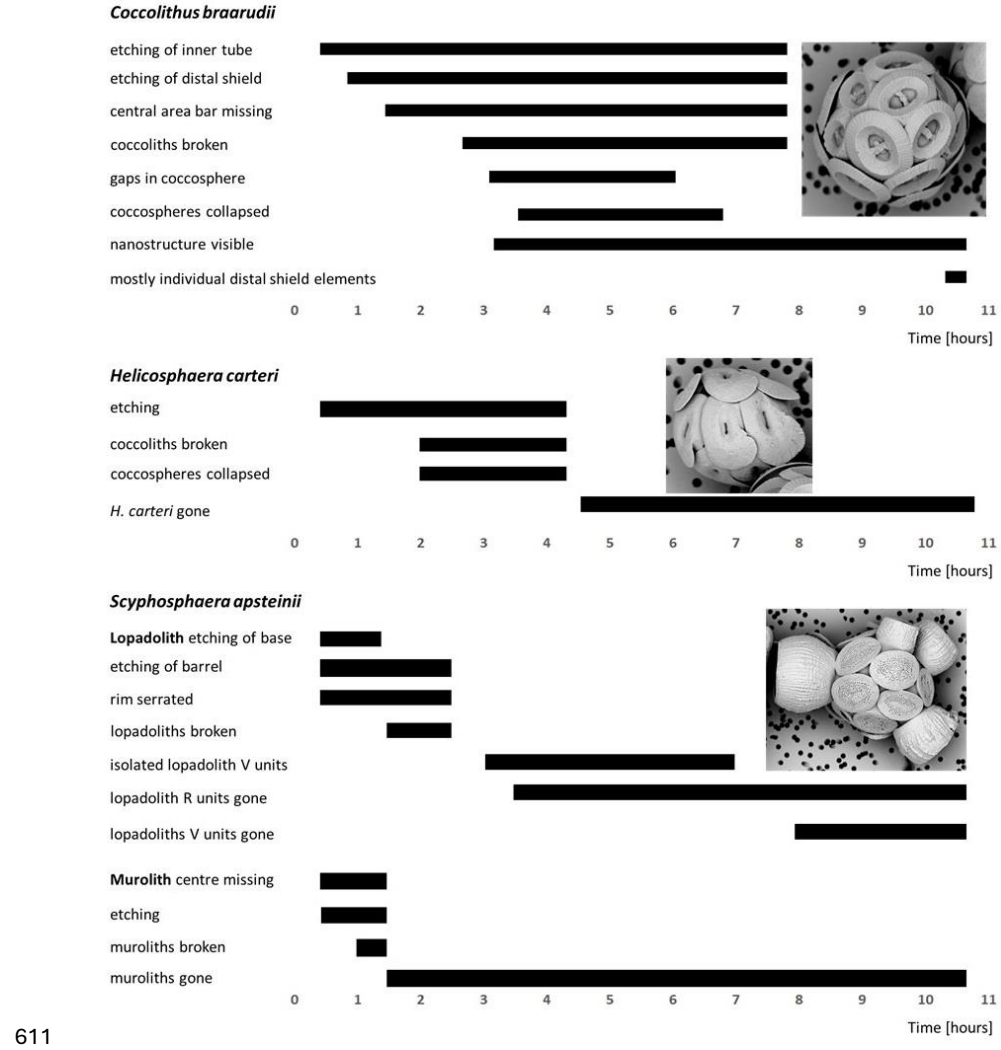

611

612

https://doi.org/10.5194/egusphere-2025-1921
Preprint. Discussion started: 25 June 2025

Fig 6 Timelines of dissolution. Bars indicate the period during which the respective feature can be observed. For example-images of each feature see Figs 1-5.

https://doi.org/10.5194/egusphere-2025-1921
Preprint. Discussion started: 25 June 2025

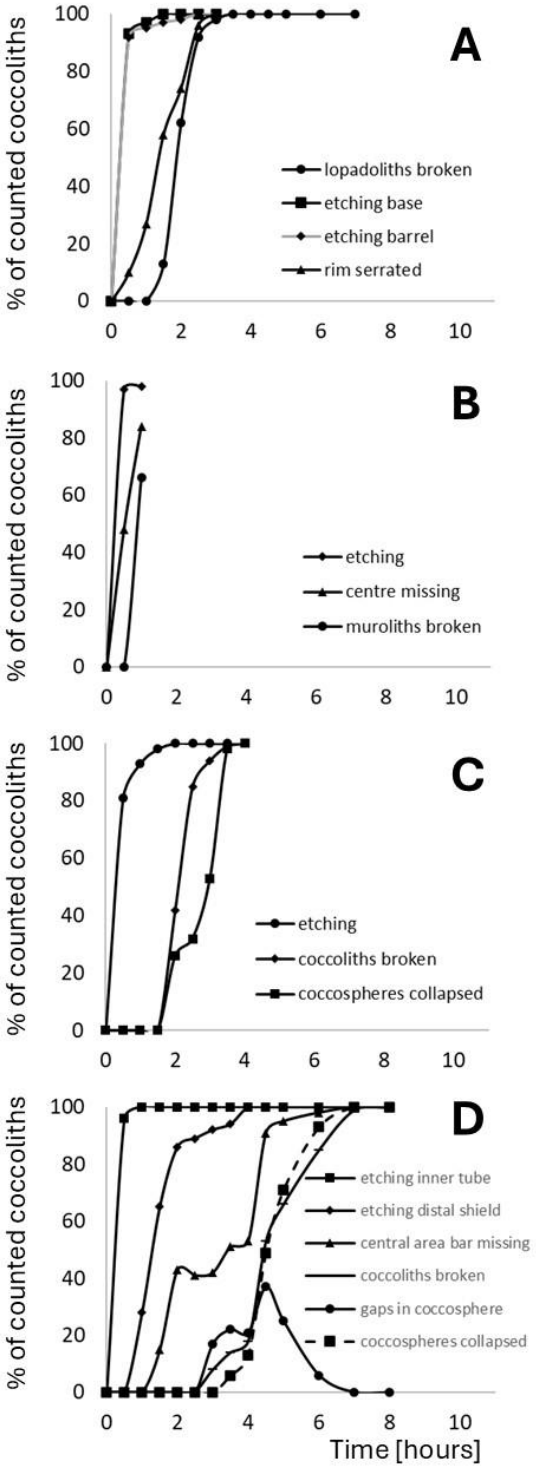

617

https://doi.org/10.5194/egusphere-2025-1921
Preprint. Discussion started: 25 June 2025

618 Fig 7 Quantification of the observations illustrated in Fig 6. Plotted is the percentage of
619 each analysed feature versus time in hours from start of experiment. A) *Scyphosphaera*
620 *apsteinii* lopadoliths B) *Scyphosphaera apsteinii* muroliths C) *Helicosphaera carteri* D)
621 *Coccolithus braarudii*

622

623

https://doi.org/10.5194/egusphere-2025-1921
Preprint. Discussion started: 25 June 2025

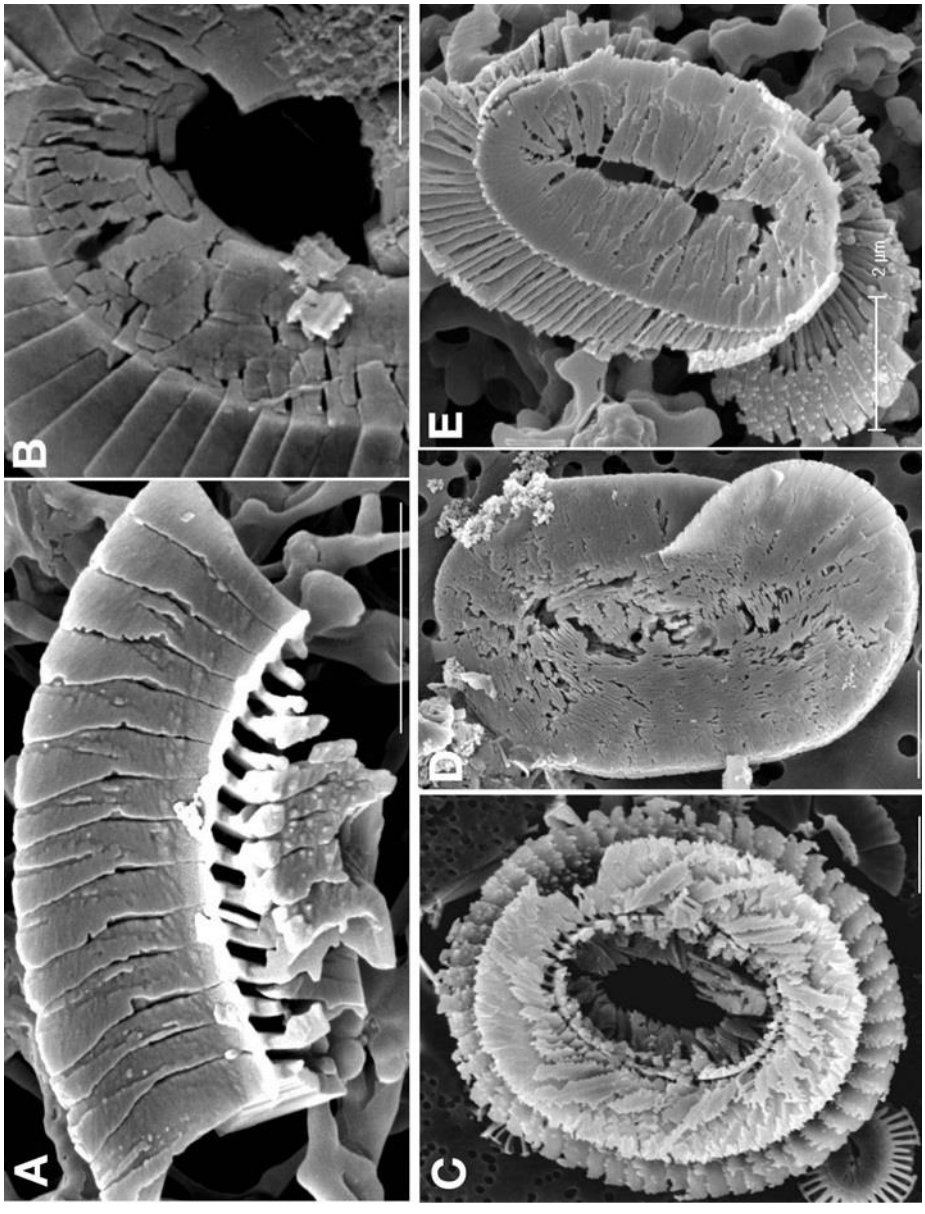

624

https://doi.org/10.5194/egusphere-2025-1921
Preprint. Discussion started: 25 June 2025

Fig 8 Field samples showing etching patterns comparable to those seen in the experimental samples. All scale bars 2 µm.

Coccolithus braarudii: A) Lower surface of a broken piece of distal shield showing nanostructure. B) Central area of distal shield showing early stage dissolution. C) Proximal surface showing advanced dissolution.

Helicosphaera carteri: D) Distal Surface showing early stage dissolution. E) Proximal surface showing advanced dissolution.